Calcoque: a Fully 3D Ship Hydrostatic Solver

François Grinnaert, *French Naval Academy Research Institute*, francois.grinnaert@ecole-navale.fr

Jean-Yves Billard, *French Naval Academy Research Institute*, jean-yves.billard@ecole-navale.fr

Jean-Marc Laurens, ENSTA Bretagne, Jean-Marc.LAURENS@ensta-bretagne.fr

ABSTRACT

Calcoque is a 3D hydrostatic computer code developed at the French Naval Academy. It computes equilibrium, stability and bending moment. A matrix algorithm transforms the classical representation of the ship by stations into a volume mesh made of tetrahedrons, prisms and hexahedrons, which can have large dimensions without degradation of the numerical result. At present the codes can handle the existing IMO intact stability criteria. It can also compute damage stability. The software code has a geometric equilibrium algorithm compatible with a strong coupling between the heel and trim. The balance position is determined on calm water and on static waves with two or three degrees of freedom. These characteristics make the code fully compatible with the second generation intact stability criteria. After some particularities of the code are presented, the paper shows a sample of computation applied to the pure loss of stability failure mode.

Keywords: *Equilibrium, algorithm, volume mesh, second generation intact stability criteria, pure loss of stability*

1. INTRODUCTION

Calcoque is a 3D hydrostatic computer code developed at the French Naval Academy for academic and research use. It computes equilibrium, stability (intact and damage) and bending moment and can handle the existing IMO intact stability criteria. It uses an unusual 3D volume method for hydrostatic computations based on meshes made of tetrahedrons, prisms and hexahedron.

The goal of this study is to use this 3D hydrostatic volume method to compute first and second level pure loss of stability criteria for a passenger ship. These criteria are extracted from IMO second generation intact stability regulation currently under development and validation (Bassler, et al., 2009, Francescutto, et. al., 2010, Wandji, et al., 2012). In order to avoid any assumption about the height of the centre of gravity, the criteria are evaluated through KG_{max} curves they generate.

This paper presents the 3D hydrostatic volume method and its application on pure loss of stability criteria.

2. VOLUME HYDROSTATIC COMPUTATION

The hydrostatic solver consists of three main algorithms. The first one transforms a classical representation of the ship by sections into a volume mesh. The second algorithm is cutting the volume mesh by a plane, generating two volume sub-meshes (one on each side of the plane) and a surface mesh at the intersection. The third one searches the balance position of the ship on calm water and on static waves with three degrees of freedom (sinkage, heel, trim) or two degrees of freedom (fixed heel). These algorithms are partially described

in a handbook (Grinnaert & Laurens, 2013) but have never been introduced in open literature. They are described below.

2.1 Generation of Volume Mesh

The ship is designed with stations, which are a list of (Y, Z) points with the same longitudinal coordinate X. Stations must be ordered from aft to forward. They are symmetrical, defined on port side only. The first point of each station is on the ship's centreline (Y=0). Vertical coordinate of the points are increasing ($Z_{i+1} > Z_i$).

Lines defined by the user connect some points of stations in order to represent the main edges of the hull. A line starts at any station and ends at any other one located forward. It has a unique point on each station it intersects and cannot miss out any station. Two lines can intersect only at a station point.
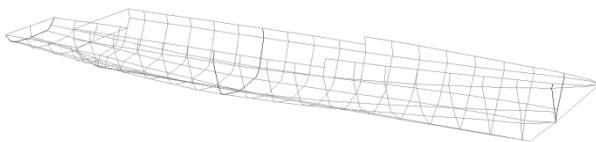

Figure 1 Stations and lines of an offshore patrol vessel.

Stations and lines (Figure 1) are used to generate a volume mesh of the ship through a "matrix" algorithm which builds the N-1 strips defined by the N stations. For each strip between stations indexed i and i+1, the process is organized in two steps.

First step. The first step consists of the generation of a matrix defining the links between all the points of the station i and all the points of station i+1. Let us consider a strip defined by a aft station with 5 points (port side only) and a forward station with 4 points. Let us consider 3 user lines. The first one links point 1 of the rear station to point 1 of the forward station (keel line). The second links point 2 (rear) to point 3 (forward). The third links point 5 (rear) to point 4 (forward). The

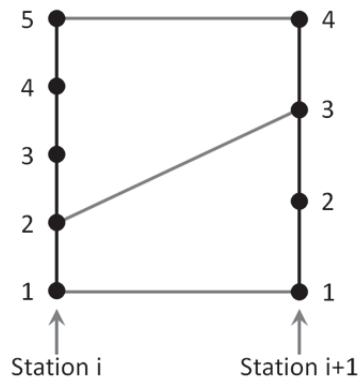strip and its links can be represented by Figure 2 (stations in black, lines in grey).

Figure 2 Strip defined by two stations and three lines.

Thus, a link matrix is defined with 5 rows associated with the 5 points of the rear station, and 4 columns associated with the 4 points of the forward station. The three user lines are represented in this matrix by three black dots in the appropriate cells (Figure 3).
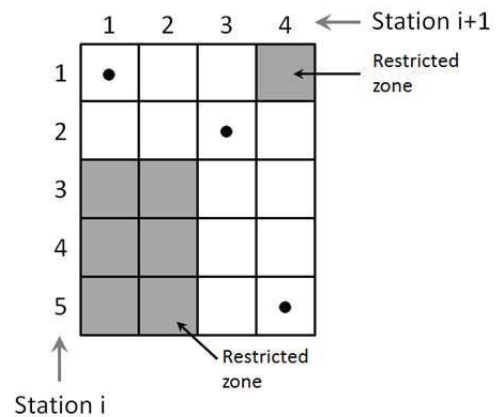

Figure 3 Link matrix associated with the strip.

Each link in the matrix defines two restricted zones which are the upper right cells and the lower left cells. This avoids considering a line which crosses another. In the current sample, the restricted zones defined by the second link (2-3) appear in grey in Figure 3. Both other links (1-1 and 5-4) define no restricted zone.

Thus, the matrix filled with user links is automatically completed with other links by going from the upper left corner to the lower right corner without missing out any cells

while passing by all cells associated with user links. Diagonal path is favoured (link 1-1 to link 2-2). If not possible, the path is horizontal (2-2 to 2-3) or vertical (3-4 to 4-4). These added links are grey dots in the left part of Figure 4. They can be added on the strip diagram (right).
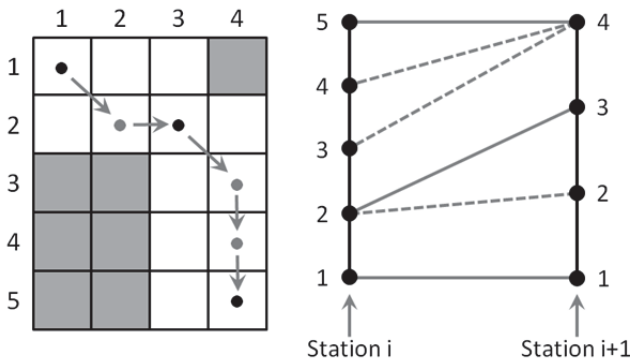

Figure 4 Completed link matrix (left) and associated strip diagram (right).

Second step. The second step consists of the generation of the volume and surface meshes defined by the completed link matrix. A diagonal path (1-1 to 2-2 and 2-3 to 3-4) generates a tetragon on each side of the hull and a hexahedron which connects both together. A horizontal path (2-2 to 2-3) generates a triangle on each side of the hull and a prism, whose bases are on the forward station. A vertical path (3-4 to 4-4 and 4-4 to 4-5) also generates two triangles and one prism, but their bases are on the rear station. The surface mesh associated with the current sample is shown in Figure 5.
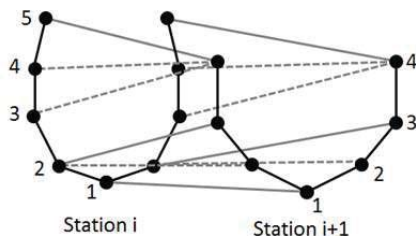

Figure 5 3D wireframe view of the strip and its surface mesh.

Flat volumes should be eliminated (same Z coordinate of the points). Some volumes may be simplified: in the sample, the first

hexahedron is a prism because the Y coordinate of the first point of each station is null.

The volume mesh of the entire ship is created by concatenating all strips (Figure 6). The volume mesh may be corrected to represent the real hull. It may be cut at the watertight deck and the void spaces (bow thruster tunnel, water inlets, flooded rooms for damage stability …) may be extracted. Both operations need a routine which cuts the mesh by a plane, described below. Volume meshes of appendages and propellers may be added.
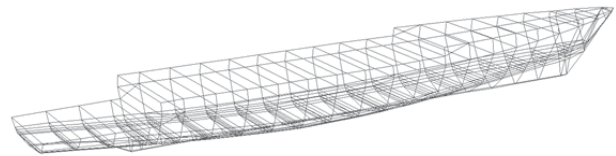

Figure 6 Wireframe view of the volume mesh of an offshore patrol vessel.

2.2 Cutting the Volume Mesh by a Plane

Cutting a volume mesh by a plane is necessary to define the waterplane. It also permits to extract some volumes from the hull (void spaces or flooded rooms) and to define volume meshes of the compartments and surface meshes of the decks. The volume mesh is made of prisms and hexahedrons. The former can be divided in three tetrahedrons and the latter in two prisms or six tetrahedrons. The cutting routine of prisms and hexahedrons only handles simple cases: volume entirely on one side or the other of the plane, a face contained in the plane or face "parallel" to the plane. In other cases, the volume being cut is previously decomposed into three or six tetrahedrons. Each point of the tetrahedron can be located on one side of the plane, included in the plane, or on the other side. Then, we have $3^4 = 81$ possibilities. However, the order of points having no importance (unlike the necessary orientation of the vertices of a surface mesh) the number of possibilities is reduced to 15 and may be simplified to 8 (see Table 1).

Case	Topology
A	No point on the upper side 1 tetrahedron on the lower side 1 intersecting triangle if 3 points in the plane
B	No point on the lower side 1 tetrahedron on the upper side
C	2 points on the upper side 2 points on the lower side 1 prism on the upper side 1 prism on the lower side 1 intersecting tetragon
D	1 point on the upper side 3 points on the lower side 1 tetrahedron on the upper side 1 prism on the lower side 1 intersecting triangle
E	3 points on the upper side 1 point on the lower side 1 prism on the upper side 1 tetrahedron on the lower side 1 intersecting triangle
F	1 point on the upper side 1 point in the plane 2 points on the lower side 1 tetrahedron on the upper side 1 tetrahedron on the lower side 1 intersecting triangle
G	2 points on the upper side 1 point in the plane 1 point on the lower side 1 tetrahedron on the upper side 1 tetrahedron on the lower side 1 intersecting triangle
H	1 point on the upper side 2 points in the plane 1 point on the lower side 1 tetrahedron on the upper side 1 tetrahedron on the lower side 1 intersecting triangle

Table 1 Cut cases of a tetrahedron with a plane.

2.3 Research of the Balance Position

The research algorithm for the balance position is partially presented in a handbook (Grinnaert & Laurens, 2013). A second method has since been implemented in the Calcoque software.

Definition of the Balance Position. The three degrees of freedom are sinkage (e, metre), heel (φ, radian) and trim (θ, radian). Sinkage replaces draught which has no sense while heel approaches 90 degrees. Sinkage is defined as the algebraic distance between a ship fixed point Q (coordinates $L_{PP}/2$, 0, Z of the reference waterline 10H) and its projected point P on the calm water waterplane (even for computation on static waves). See Figure 7.
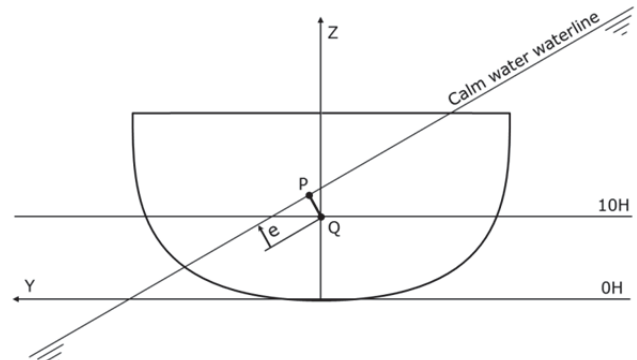

Figure 7 Sinkage.

Balance is achieved if the three following conditions are met:

$$\varepsilon_\nabla = \nabla_0 - \nabla = 0 \qquad (1.1)$$

$$\varepsilon_x = 0 \qquad (1.2)$$

$$\varepsilon_y = 0 \qquad (1.3)$$

With:
∇ Computed displacement volume (m^3)
∇_0 Ship displacement volume (m^3)
ε_∇ Volume gap (m^3)
ε_X Longitudinal gap (m, defined below)
ε_Y Transverse gap (m, defined below)

Heel can be free (research of the balance position) or fixed (GZ curve computation). In that case, the third condition is ignored and the transverse gap ε_Y is the righting arm lever GZ.

Inclined Ship Planes. ε_X and ε_Y gaps are respectively the algebraic longitudinal and transverse distances between the centre of gravity (G) and the Earth vertical through the centre of buoyancy (B). Two "inclined ship planes" are defined to compute these gaps. Their line of intersection is the Earth vertical whose director vector is $\mathbf{n_1}$.

The transverse plane of inclined ship also contains vector $\mathbf{n_2}$ defined as:

$$\mathbf{n_2} = \frac{\mathbf{n_1} \wedge \mathbf{X}}{\|\mathbf{n_1} \wedge \mathbf{X}\|} \quad (2)$$

The longitudinal plane of inclined ship contains $\mathbf{n_1}$ and $\mathbf{n_3}$ vectors with:

$$\mathbf{n_3} = \mathbf{n_2} \wedge \mathbf{n_1} \quad (3)$$

In the ship fixed coordinates system, the three vectors are:

$$
\begin{aligned}
n_{1.x} &= -\sin\theta \\
n_{1.y} &= -\sin\varphi\,\cos\theta \\
n_{1.z} &= \cos\varphi\,\cos\theta
\end{aligned}
\quad (4.1)
$$

$$
\begin{aligned}
n_{2x} &= 0 \\
n_{2.y} &= \cos\varphi \\
n_{2.z} &= \sin\varphi
\end{aligned}
\quad (4.2)
$$

$$
\begin{aligned}
n_{3x} &= \cos\theta \\
n_{3.y} &= -\sin\varphi\,\sin\theta \\
n_{3.z} &= \cos\varphi\,\sin\theta
\end{aligned}
\quad (4.3)
$$

Thus, ε_X and ε_Y gaps are respectively the algebraic distances between G and the transverse and longitudinal planes of the inclined ship. They are computed as follows:

$$\varepsilon_x = \mathbf{BG}.\,\mathbf{n_3} \quad (5.1)$$

$$\varepsilon_y = GZ = \mathbf{BG}.\,\mathbf{n_2} \quad (5.2)$$
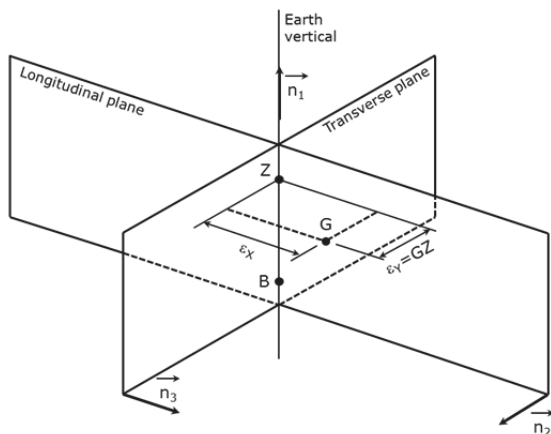
Gaps and planes are shown in Figure 8.

Figure 8 Gaps and inclined ship planes.

This expression of the longitudinal gap is more accurate than the simplified strip method proposed by the SLF 52/INF.2 (annex 6) which consists in:

$$LCB = LCG \quad (6)$$

Hydrostatic computation on calm water. The waterplane, depending on sinkage (e), heel (φ) and trim (θ), is defined with a point P (see Figure 7) and the vector $\mathbf{n1}$ with:

$$\mathbf{QP} = e.\,\mathbf{n_1} \quad (7)$$

When searching for the balance position, the displacement volume (∇) and its centre (B) are computed by cutting the watertight volume mesh by the waterplane.

Hydrostatic computation on waves. Watertight volume is previously divided in strips by cutting with transverse planes. SLF 52/INF.2 (annex 6) recommends at least 20 strips. In each strip, the following are defined (see Figure 9):
- Plane P_1: strip's rear plane.
- Plane P_2: strip's forward plane.
- Line D_3: through point P with director vector $\mathbf{n_3}$ (longitudinal line included in the calm waterplane).
- Point I_1: intersection of P_1 and D_3.
- Point I_2: intersection of P_2 and D_3.

Three points (A, B and C) define the strip's local waterplane. They are defined as follows (see Figure 9):

$$\mathbf{OA} = \mathbf{OI_1} + \mathbf{n_2} + z_1.\,\mathbf{n_1} \quad (8.1)$$

$$\mathbf{OB} = \mathbf{OI_1} - \mathbf{n_2} + z_1.\,\mathbf{n_1} \quad (8.2)$$

$$\mathbf{OC} = \mathbf{OI_2} + z_2.\,\mathbf{n_1} \quad (8.3)$$

With:

$$z_1 = \frac{h}{2}\cos(k.\,x_1 + \Phi) \quad (9.1)$$

$$z_2 = \frac{h}{2}\cos(k.\,x_2 + \Phi) \quad (9.2)$$

$$\Phi \in [0, 2\pi[$$

h   Wave height (m)

k   Wave number (m^{-1})

x_1 Longitudinal position of the rear plane of the strip

x_2 Longitudinal position of the forward plane of the strip
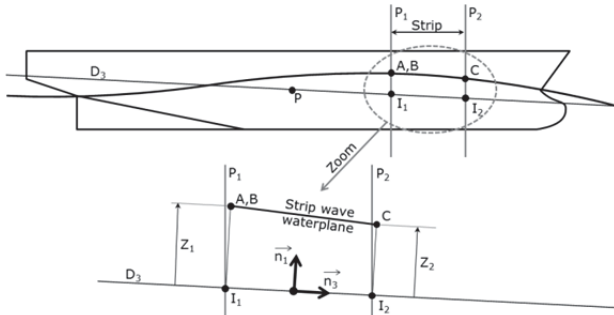

Figure 9 Strip wave waterplane.

Balance - First Method. The process is iterative. At each step, three gaps (two if fixed heel) are computed as explained above. Sinkage, heel and trim are corrected as follows before being used in the next step:

$$e_{i+1} = e_i + \frac{\varepsilon_\nabla}{A_{WP}} \quad (10.1)$$

$$\varphi_{i+1} = \varphi_i + \frac{\varepsilon_y}{|GM_T|} \quad (10.2)$$

$$\theta_{i+1} = \theta_i + \frac{\varepsilon_x}{|GM_L|} \quad (10.3)$$

With:

e_i sinkage at step i (m)

e_{i+1} sinkage at step i+1 (m)

φ_i heel at step i (rad)

φ_{i+1} heel at step i+1 (rad)

θ_i trim at step i (rad)

θ_{i+1} trim at step i+1 (rad)

Absolute values of the metacentric heights permit to let the process diverge in case of transverse or longitudinal instability. At first step, the waterplane area (A_{WP}) and metacentric heights (GM_T, GM_L) may be calculated with the hydrostatic table or by direct computation on the waterplane surface mesh, which must be projected on an Earth-horizontal plane in case of computation on waves. At next steps, they are computed as follows:

$$A_{WP} = \frac{\nabla_{i+1} - \nabla_i}{e_{i+1} - e_i} \quad (11.1)$$

$$GM_T = \frac{\varepsilon_{y.i+1} - \varepsilon_{y.i}}{\varphi_{i+1} - \varphi_i} \quad (11.2)$$

$$GM_L = \frac{\varepsilon_{x.i+1} - \varepsilon_{x.i}}{\theta_{i+1} - \theta_i} \quad (11.3)$$

When the three gaps (ε_∇, ε_φ, ε_θ) are small enough, the balance position is considered reached. This method is compatible with a strong coupling between the heel and trim (unconventional floating structures). However, it is fragile if the coupling between the trim and sinkage is strong because the corrections of trim and sinkage may conflict.

Balance - Second Method. This method is also iterative and has been developed after the publication of the handbook (Grinnaert & Laurens, 2013). Before the iterative process, an initial hydrostatic computation gives the three gaps for initial values of e, θ and φ. At each step of the iterative process, three hydrostatic computations (two if fixed heel) are performed. They permit to evaluate separately the influence of a small increment of sinkage, heel and trim on the values of the three gaps. These computations are listed in Table 2.

	Input data			Output data		
1	$e+\varepsilon_e$	θ	φ	$\varepsilon_{\nabla e}$	ε_{xe}	ε_{ye}
2	e	$\theta+\varepsilon_\theta$	φ	$\varepsilon_{\nabla\theta}$	$\varepsilon_{x\theta}$	$\varepsilon_{y\theta}$
3	e	θ	$\varphi+\varepsilon_\varphi$	$\varepsilon_{\nabla\varphi}$	$\varepsilon_{x\varphi}$	$\varepsilon_{y\varphi}$

Table 2 Hydrostatic computations.

With:

ε_e $d_{full}/100$ small sinkage increment

ε_θ 0.1 degree   small trim increment

ε_e 1.0 degree   small heel increment

d_{full} (m)   full loaded ship draught

Then, still in the same iteration, the following system of three equations with three unknowns (2x2 if fixed heel) is solved:

$$\begin{pmatrix} \dfrac{\varepsilon_{\nabla e} - \varepsilon_{\nabla}}{\varepsilon_e} & \dfrac{\varepsilon_{\nabla\theta} - \varepsilon_{\nabla}}{\varepsilon_\theta} & \dfrac{\varepsilon_{\nabla\varphi} - \varepsilon_{\nabla}}{\varepsilon_\varphi} \\[3mm] \dfrac{\varepsilon_{xe} - \varepsilon_x}{\varepsilon_e} & \dfrac{\varepsilon_{x\theta} - \varepsilon_x}{\varepsilon_\theta} & \dfrac{\varepsilon_{x\varphi} - \varepsilon_x}{\varepsilon_\varphi} \\[3mm] \dfrac{\varepsilon_{ye} - \varepsilon_y}{\varepsilon_e} & \dfrac{\varepsilon_{y\theta} - \varepsilon_y}{\varepsilon_\theta} & \dfrac{\varepsilon_{y\varphi} - \varepsilon_y}{\varepsilon_\varphi} \end{pmatrix} \times \begin{pmatrix} de \\[3mm] d\theta \\[3mm] d\varphi \end{pmatrix} = \begin{pmatrix} -\varepsilon_{\nabla} \\[3mm] -\varepsilon_x \\[3mm] -\varepsilon_y \end{pmatrix}$$

Unknowns are de, dθ and dφ, which are increments of sinkage, trim and heel to be added at current values to cancel the gaps. The second and third terms of the diagonal are respectively the longitudinal and transverse metacentric heights. Their sign may be used to detect instability and invert the sign of the trim and heel increments.

At the end of the iteration, a last hydrostatic computation is done using corrected values of sinkage, trim and heel. If the three gaps are small enough, the balance position is considered reached.

This second method is as suitable as the first for a strong coupling between the heel and trim. It is more robust in case of strong coupling between the trim and sinkage. The number of iterations is very small (1 or 2, see Table 3) but the number of hydrostatic computations is similar. If n is the number of iterations, the number of hydrostatic computations is 3n + 1 if the heel is fixed and 4n + 1 if it's free.

Comparison of Methods. Table 3 shows the GZ computed for a 13,000-ton ferry (length 160 m) using both methods. It also shows numbers of iterations and hydrostatic computations to reach each balance position with fixed heel. The maximum allowed gaps are 1 m^3 in volume and 1 millimetre for ε_x. The maximum difference between both GZ is lower than 0.02 millimetres.

Heel (deg.)	First method			Second method		
	GZ (m)	Nb. iter.	Nb. calc.	GZ (m)	Nb. iter.	Nb. calc.
0	0.000	8	8	0.000	2	7
1	0.042	6	6	0.042	1	4
2	0.085	7	7	0.085	1	4
3	0.130	11	11	0.130	1	4
4	0.176	7	7	0.176	1	4
5	0.224	7	7	0.224	1	4
10	0.484	8	8	0.484	2	7
15	0.774	8	8	0.774	2	7
20	1.103	8	8	1.103	2	7
25	1.441	7	7	1.441	2	7
30	1.737	8	8	1.737	2	7
35	1.984	5	5	1.984	2	7
40	2.179	5	5	2.179	2	7
45	2.252	6	6	2.252	2	7
50	2.189	6	6	2.189	2	7
Sum			107	Sum		90

Table 3 Comparison of both balance methods.

Transverse metacentric height computation. The transverse metacentric height is computed using two first points of the GZ curve (0 and 1 degree).

$$GM_T = \left(\frac{dGZ}{d\varphi}\right)_{\varphi=0} \qquad (13)$$

In the case of the hydrostatic computation on waves, the inertia of the projected waterplane is not used as recommended in the simplified strip method proposed by the IMO (see SLF 52/INF.2 annex 6).

3. APPLICATION TO THE PURE LOSS OF STABILITY FAILURE MODE

3.1 Goal and Ship Presentation

The volume method is applied to compute the first and the second level of pure loss of stability criteria for a ferry whose characteristics are shown in Table 4. These criteria are extracted from second generation intact stability criteria, which are currently under development and validation at the IMO.

They are thoroughly presented by Umeda (2013). Two methods are proposed for the level one criterion. The first method considers a parallel waterplane with lowest draught (d_L). The second method consists in minimum GM_T computation on a static sinusoidal wave which has the same length as the ship. Both methods are tested. No assumption of centre of gravity position is made. KG_{max} curves are computed for several displacements with zero trim. Two watertight volumes are considered, respectively limited at 14 m and 9 m above base line. Their meshes include appendages. Void spaces are truncated (bow thruster's tunnel and retractable stabilizers' housings).

Length overall	L_{OA}	175 m
Length between perpendiculars	L_{PP}	160 m
Breadth	B	24 m
Full load displacement	Δ	13147 tons
Draught	d_{full}	6.00 m
Froude number @ 25 knots	Fn	0.325

Table 4 Ship main characteristics.

3.2   Watertight volume limited at 14 m

KG_{max} curves for the first and the second level of pure loss of stability criteria are shown in Figure 10.

First level. Both methods proposed for the first level give significantly different results. The first is quite more conservative than the second. The curve associated with first method has a hook at a draught of 5.67 m, which is the consequence of a loss of inertia on the parallel waterplane due to the stabilizers housings (see dark grey waterplane in Figure 11). Using the theoretical hull would mask this phenomenon.

Recommendation: Regulation   should specify the hull to use (real or bare). It should be noted that the simplified strip method proposed by the SLF 52/INF.2 annex 6 is not compatible with a real hull. This simplified method has been used by Wandji and Corrignan to apply the second generation criteria on a large sample of ships (Wandji, et al., 2012).
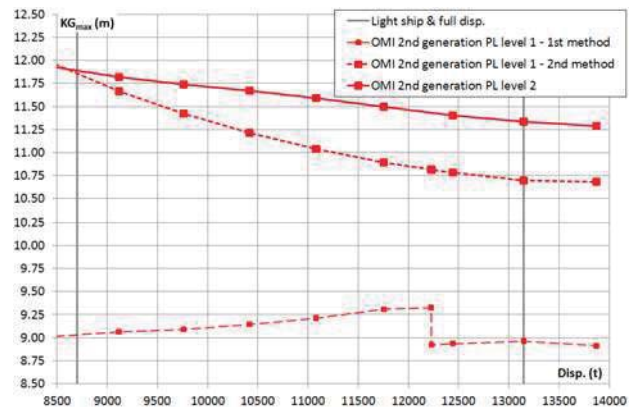

Figure 10 KG_{max} curves associated with 1st and 2nd level pure loss of stability criteria.

Figure 11   Parallel waterplanes for d=6.00 m (light grey) and d_L=3.33 m (dark grey).

Second level. We observe that the second level criterion is less conservative than both first level methods (except for one point below light ship displacement).

Comparison with first generation criteria. KG_{max} curves associated with first and second generation criteria are compared in Figure 12. We observe that the pure stability loss criteria do not introduce a higher requirement for this ship. The existing ship will comply with the new regulation but the architect will need to compute the second level criterion to prove it.
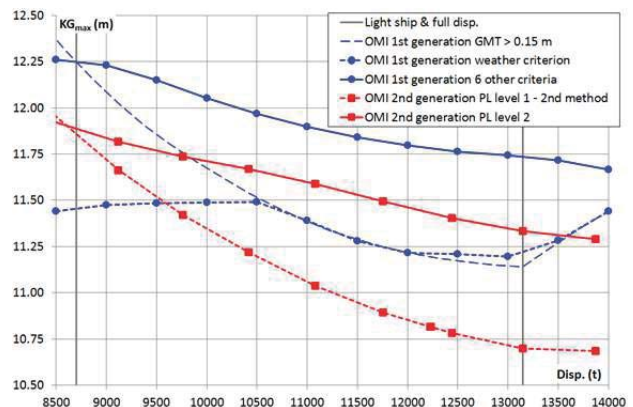

Figure 12 Comparison of 1st and 2nd generation criteria KG_{max} curves.

3.3 Influence of watertight deck height

The watertight deck is lowered from 14 to 9 metres.

First level. Lowering the watertight deck has normally no influence on the first level criterion which considers only metacentric height (hence small inclinations). For the first method (parallel waterplane at lowest draught), this is evident. For the second method (GM computation on wave), the wave crest should pass over the watertight deck, reducing the waterplane and its inertia. This situation does not occur with the watertight deck at 9 m (freeboard at full load is 3 m, to be compared with wave half-height which is 2.67 m). However, it appears at a draught over 6 m if the watertight deck is lowered at 8 m (in this case the ship does not comply with the current regulation). See KG_{max} curves in Figure 13.
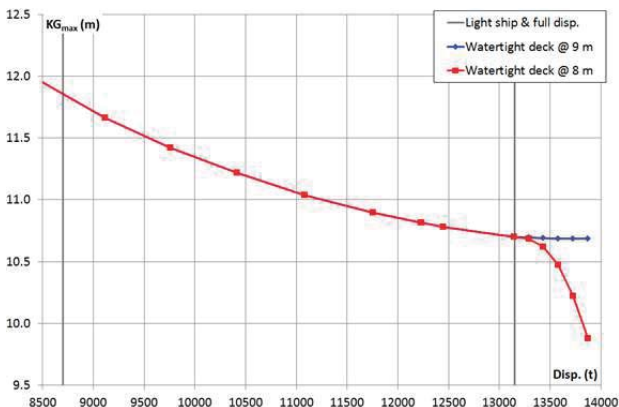

Figure 13 KG_{max} curves for 1st level criterion (2nd method) for watertight deck at 9 and 8 m.

The situation for the last point of the curve "Watertight deck @ 8 m" in Figure 13 (d=6.25 m) is shown in Figure 14. The waterplane is truncated on a quarter of its length. This situation should not occur in reality because the wave crest should not flood the garage deck even if its volume is considered as not watertight.
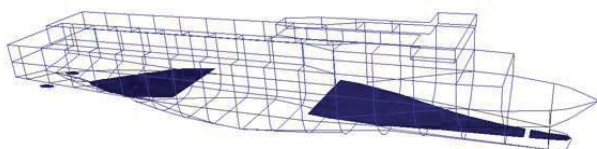

Figure 14 Truncated waterplane.

Recommendation: Regulation should specify the watertight volume to use. French military regulation (IG6018A) considers two different watertight volumes. The "bulkhead deck" is its upper limit which is tight to prolonged immersion. This watertight volume is considered in damage stability. In this sample, this deck should be the garage deck at 8 or 9 m above baseline. The "weather deck" is the upper limit which is tight to non-prolonged immersion. It may be the bulkhead deck or above. The increased watertight volume associated with this deck is considered in intact stability. In this sample, this deck should be located at 14 m above baseline (first passenger deck).

Second level. KG_{max} curves associated with the second level criterion for the lowered watertight volume height are shown in Figure 15. They are compared to those associated with the first level (independent from the watertight volume height) and those associated with the first generation criteria recalculated for the same watertight volume. As before, we observe that the pure loss of stability criteria do not introduce any additional requirement compared to first generation criteria. However, we note that the second level criterion is more demanding than the first level criterion calculated by the second method (GM computation on wave). This is a paradoxical situation.
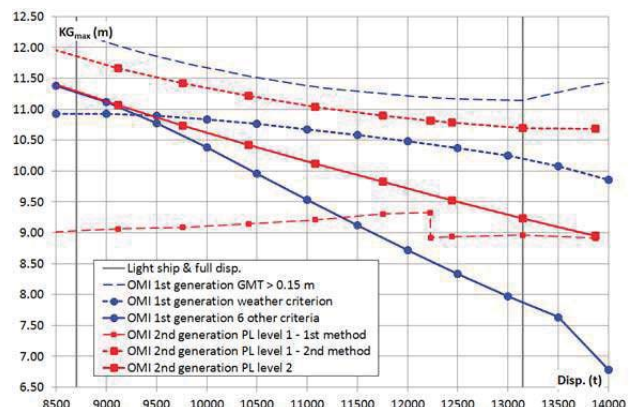

Figure 15 KG_{max} curves for a watertight volume limited at 9 m.

Figure 16 compares the KG_{max} curves associated with pure loss of stability criteria first and second level computed for both watertight decks located at 9 m and 14 m from baseline.
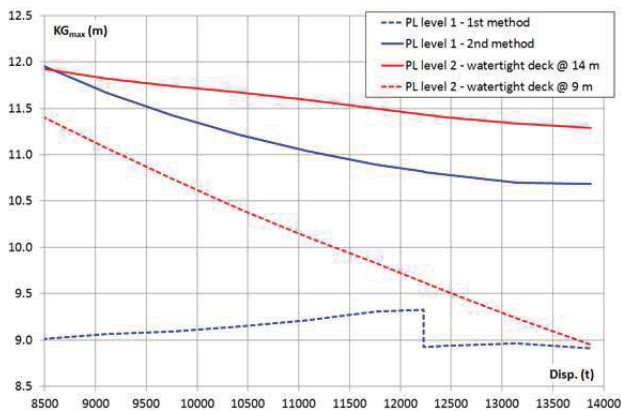

Figure 16 Influence of the watertight volume height on pure loss of stability KG_{max} curves.

4. CONCLUSION

The 3D hydrostatic volume code implemented in the Calcoque software is fully compatible with the first and second level pure loss of stability criteria. It can handle the real hull of the ship, with its appendages and void spaces. Use of this code to compute KG_{max} curves of a passenger ship showed:

▪ New requirements regarding pure loss of stability criteria are similar to those of the first generation criteria.
▪ The importance of a rigorous definition of the watertight volume to be considered (real or bare hull, upper limit).
▪ A paradoxical situation when the watertight deck is lowered (first level requires more than second level).

The study should be continued with other civilian and military ships of different geometries and extended to parametric roll, whose hydrostatic computations are similar to those of pure loss of stability.

5. REFERENCES

Bassler, C., Belenky, V., Bulian, G., Francescutto, A., Spyrou, K., Umeda, N., "A Review of Available Methods for Application to Second Level Vulnerability Criteria", Proceedings of the 10th International Conference on Stability of Ships and Ocean Vehicles, pp. 111-128, 2009.

Direction Générale de l'Armement, "Stabilité des bâtiments de surfaces de la Marine Nationale", IG6018A, 1999, Restricted diffusion.

Francescutto, A., Umeda, N., "Current Status of New Generation Intact Stability Criteria Development", Proceedings of the 11th International Ship Stability Workshop, pp 1-5, 2010.

Grinnaert, F., Laurens, J.-M., Stabilité du navire – Théorie, réglementation, méthodes de calcul – Cours et exercices corrigés, ISBN 978-2-7298-80644, Ellipses, 2013.

SLF 52/INF.2, "Information collected by the intersectional Correspondence Group on Intact Stability", Submitted by USA, IMO, London, 2009.

Umeda. N., "Current Status of Second Generation Intact Stability Criteria Development and Some Recent Efforts", Proceedings of the 13th International Ship Stability Workshop, pp 138-157, 2013.

Wandji. C., Corrignan. P., "Test Application of Second Generation IMO Intact Stability Criteria on a Large Sample of Ships", Proceedings of the 11th International Conference on the Stability of Ships and Ocean Vehicles, pp 129-139, 2012.